JOC Article

Mechanistic and Kinetic Insights into the Thermally Induced Rearrangement of α-Pinene

Achim Stolle,*,† Bernd Ondruschka,† and Matthias Findeisen‡

Institute for Technical Chemistry and Environmental Chemistry, Friedrich-Schiller University Jena, Lessingstr. 12, D-07743 Jena, Germany, and Institute for Analytical Chemistry, University Leipzig, Linnéstr. 3, D-04103 Leipzig, Germany

achim.stolle@uni-jena.de

Received June 17, 2008

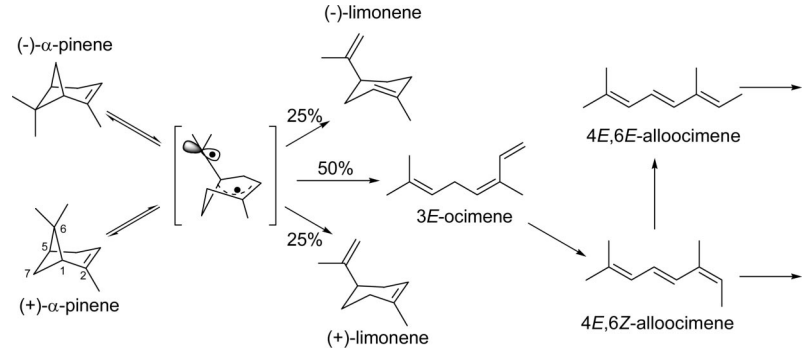

The thermal rearrangement of α-pinene (**1**) is interesting from mechanistic as well as kinetic point of view. Carrier gas pyrolyses with **1** and its acyclic isomers ocimene (**2**) and alloocimene (**3**) were performed to investigate the thermal network of these hydrocarbons. Kinetic analysis of the major reaction steps allows for a deeper insight in the reaction mechanism. Thus it was possible to explain the racemization of **1**, the formation of racemic limonene (**4**), and the absence of the primary pyrolysis product **2** in the reaction mixture resulting from thermal rearrangement of **1**. Results supported the conclusion that the reactions starting with **1** involve biradical transition states.

Introduction

The thermal isomerization of α-pinene (**1**) is a long-known, deeply investigated reaction.[1] First studies were published in the 1930s by Smith and Carlson, who independently observed racemization of the pyrolysis products yielded by thermal treatment of **1**.[2] The authors believed that this was due to the formation of racemic limonene (**4**, dipentene; Scheme 1). More intensive studies revealed that beside the rearrangement of **1** to alloocimene (**3**) and **4** the pyrolysis of **1** yields nonconverted α-pinene with a lower optical activity as found for the starting material.[2−5] Apparently, the initial formation of a biradical was assumed as explanation of these observations (Scheme 1).[6] Due to the fact that this mechanism has to lead to the formation of ocimene (**2**) and the absence of this product in the pyrolysis mixtures was proved in different studies, a fast isomerization of **2** to **3** was proposed by various authors.[5−7] α-Pinene (**1**) has been intensively subjected to kinetic studies in both gaseous

SCHEME 1. Reaction Products Resulted from Thermal Isomerization of α-Pinene (1)

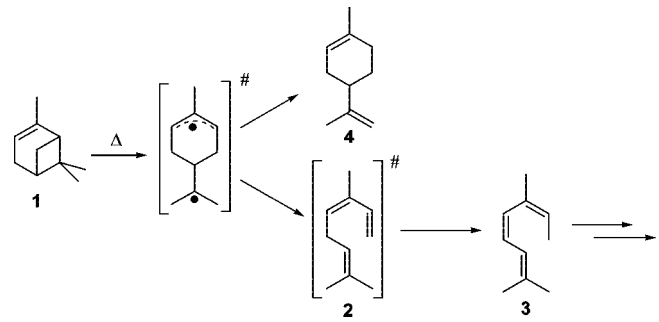

† Friedrich-Schiller University Jena.

‡ University Leipzig.

(1) (a) Egloff, G.; Herrman, M.; Levinson, B. L.; Dull, M. F. *Chem. Rev.* **1934**, *14*, 287–383. (b) Frost, A. A.; Pearson, R. G. Die Thermische Isomerisation von α- und *β*-Pinen. In *Kinetik und Mechanismus homogener chemischer Reaktionen*; Verlag Chemie: Weinheim, 1964; pp 349−354. (c) Banthorpe, D. V.; Whittaker, D. *Quart. Rev.* **1966**, *20*, 373–387. (d) Naves, Y. R. *Russ. Chem. Rev.* **1968**, *37*, 779–788.

(2) (a) Smith, D. F. *J. Am. Chem. Soc.* **1927**, *49*, 43–50. (b) Conant, J. B.; Carlson, G. H. *J. Am. Chem. Soc.* **1929**, *51*, 3464–3469.

10.1021/jo8012995 CCC: $40.75
Published on Web 09/30/2008

and condensed phase,[8−10] but the consecutive reactions of **2** and **3** are rarely investigated.[9,11] Deuterium-labeling experiments performed by Gajewski and co-workers support the hypothesis that a biradical is responsible for the formation of the primary pyrolysis products (**2**, **4**, racemic **1**) resulting from rearrangement of optically active **1**.[10] Recently, studies were published showing that isomerization of **1** can be carried out in supercritical alcohols without lost of the initial optical activity of **1** but accompanied by the formation of dipentene.[12−14]

Although many results have been published in the literature concerning the thermal isomerization of **1** already, it seems to be appropriate to investigate the pyrolysis once more from a mechanistic and kinetic point of view. Performing pyrolysis experiments with **1**, **2**, and **3** under identical conditions allows for a detailed study of the mechanisms of interconversions of these compounds. The calculation of activation parameters according to Arrhenius and Eyring on the basis of kinetic pyrolyses forces the understanding of the transition states the reactions pass through. Performing the pyrolysis experiments in a flow system at ambient pressure using nitrogen as diluting agent and carrier gas allows for calculation of rate constants apart from the falloff region.

Results and Discussion

Pyrolysis of α-Pinene. In order to unravel the complex product mixture resulting from thermal rearrangement of α-pinene (**1**), flow-type pyrolysis experiments at ambient pressure were conducted with **1** and its main isomerization products ocimene (**2**) and alloocimene (**3**). Comparative chromatograms for these experiments are given in Supporting Information. The plot of conversion of **1** and of the yields of pyrolysis products versus pyrolysis temperature (*T*) is depicted in Figure 1. With respect to the amounts of products initially formed from **1** (**2**, **4**) significant differences were found. Whereas **4** is formed with a selectivity of approximately 45%, the yield of the acyclic primary pyrolysis product **2** does not exceed 2%, pointing out that **2** is a reactive molecule that rapidly rearranges to **3**. At a pyrolysis temperature of 412 °C the yield of **3** passes through a maximum and further increase of temperature gives rise to the formation of consecutive products (**cp**, e.g. pyronene).[10] Decomposition and aromatization products of pyronenes constitute the main fraction resulting from experiments at temperatures higher than 525 °C. Interestingly, the ratio of primarily formed products **4** and **2** (including consecutive reaction products such as **3** or **cp**) practically remains constant

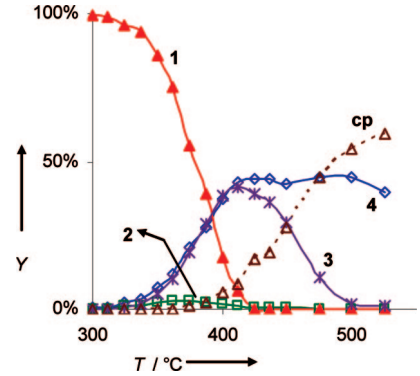

FIGURE 1. Yield of pyrolysis products of α-pinene pyrolysis and content of remaining α-pinene (**1**) depending on reaction temperature (*T*). **2**, ocimene; **3**, alloocimene; **4**, limonene; **cp**, consecutive products. 15 μL starting material; carrier gas, N_2; flow rate, 1.0 L min^{-1}; τ, 0.51−0.71 s.

within the temperature range of 350−500 °C (Figure 1). Therefore, it can be concluded that the reaction pathways starting from biradical intermediate sketched in Scheme 1 are not affected by changes in reaction temperature, which is according to Carpenter not atypical for reactions passing through a joint transition state or reaction intermediate.[15] Subjecting limonene (**4**) to pyrolysis studies at temperatures higher than 550 °C yielded aromatized products.[16,17]

The influence of reaction temperature on the enantiomeric ratio of both **1** and **4** was subject of these studies also. Pyrolysis experiments with optically pure (1*S*,5*S*)-(−)-**1** and (1*R*,5*R*)-(+)-**1** were conducted, whereby the initial enantiomeric excess (ee) values were 80% and 95%, respectively. Temperature plots of the corresponding yields of both enantiomers of **1** for pyrolysis of either (−)-**1** and (+)-**1** are pictured in Figure 2a and b, respectively, clearly indicating that pyrolyses at elevated temperatures lead to a racemization of the starting materials. Contrary to previous studies on the loss of optical activity of **1** while heating,[2] a complete racemization was not observed in both cases, because of the fact that complete conversion was reached first (425 °C). Additionally, the enantiomeric ratio of optically active pyrolysis product **4** was calculated based on GC runs using the same β-cyclodextrine column as used for the determination of relative enantiomeric yields in the case of **1**. Results shown in Figure 2 for the pyrolysis of both enantiomers of **1** reveal that in both cases a racemic mixture of (−)-**4** and (+)-**4** was formed.

Pyrolysis of Ocimene. Pyrolysis experiments with a mixture of 3*Z*- (**2a**) and 3*E*-ocimene (**2b**; Chart 1) were conducted to unravel the products formed from their thermal treatment. GC analyses showed that the ratio of the two stereoisomers of **2** was approximately 0.5 in favor of **2b**. The same results were found in the ^{1}H NMR spectrum of the mixture. Structures were confirmed by one-dimensional NOESY experiments explained in Supporting Information. Explorative pyrolyses investigating the temperature dependency of the conversion of **2** reveal differences in the thermal behavior of **2a** and **2b** pictured in Figure 3. Whereas the *Z*-isomer (**2a**) is completely converted at a pyrolysis temperature of 375 °C, **2b** is thermally stable up to 525 °C, thus indicating that pyrolysis of **1** mainly yields **2a**.

(3) (a) Goldblatt, L. A.; Palkin, S. *J. Am. Chem. Soc.* **1941**, *63*, 3517–3522. (b) Savich, T. R.; Goldblatt, L. A. *J. Am. Chem. Soc.* **1945**, *67*, 2027–2031.
(4) Fuguitt, R. E.; Hawkins, J. E. *J. Am. Chem. Soc.* **1945**, *67*, 242–245.
(5) Hawkins, J. E.; Hunt, H. G. *J. Am. Chem. Soc.* **1951**, *73*, 5379–5381.
(6) Burwell, R. L. *J. Am. Chem. Soc.* **1951**, *73*, 4461–4462.
(7) Hawkins, J. E.; Burris, W. A. *J. Org. Chem.* **1959**, *24*, 1507–1510.
(8) (a) Fuguitt, R. E.; Hawkins, J. E. *J. Am. Chem. Soc.* **1947**, *69*, 319–322. (b) Hunt, H. G.; Hawkins, J. E. *J. Am. Chem. Soc.* **1950**, *72*, 5618–5620. (c) Hawkins, J. E.; Vogh, J. W. *J. Phys. Chem.* **1953**, *57*, 902–905.
(9) Riistama, K.; Harva, O. *Finn. Chem. Lett.* **1974**, *4*, 132–138.
(10) (a) Gajewski, J. J.; Kuchuk, I.; Hawkins, C. M.; Stine, R. *Tetrahedron* **2002**, *58*, 6943–6950. (b) Gajewski, J. J.; Hawkins, C. M. *J. Am. Chem. Soc.* **1986**, *108*, 838–839.
(11) Sasaki, T.; Eguchi, S.; Yamada, H. *Tetrahedron Lett.* **1971**, *12*, 99–103.
(12) Anikeev, V. I.; Yermakova, A.; Chibiryaev, A. M.; Kozhevnikov, I. V.; Mikenin, P. E. *Russ. J. Phys. Chem. A* **2007**, *81*, 711–716.
(13) Chibiryaev, A. M.; Yermakova, A.; Kozhevnikov, I. V.; Sal'nikova, O. I.; Anikeev, V. I. *Russ. Chem. Bull. Int. Ed.* **2007**, *56*, 1234–1238.
(14) Yermakova, A.; Chibiryaev, A. M.; Kozhevnikov, I. V.; Anikeev, V. I. *Chem. Eng. Sci.* **2007**, *62*, 2414–2421.
(15) Carpenter, B. K. *J. Am. Chem. Soc.* **1985**, *107*, 5730–5732.
(16) Stolle, A.; Brauns, C.; Nüchter, M.; Ondruschka, B.; Bonrath, W.; Findeisen, M. *Eur. J. Org. Chem.* **2006**, 3317–3325.
(17) Pines, H.; Ryer, J. *J. Am. Chem. Soc.* **1955**, *77*, 4370–4375.

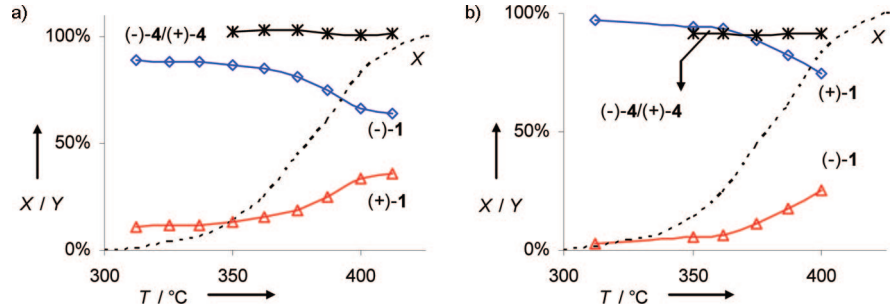

FIGURE 2. Conversion of α-pinene (*X*), relative content of (−)-α-pinene [(−)-**1**], relative content of (+)-α-pinene [(+)-**1**], and ratio of (−)- and (+)-limonene (**4**) depending on the reaction temperature (*T*) for the pyrolyses of (−)-**1** (Figure 2a) and (+)-**1** (Figure 2b). 15 μL starting material; carrier gas, N_2; flow rate, 1.0 L min^{-1}; τ, 0.60−0.70 s; enantiomeric ratios measured with a β-cyclodextrine column.

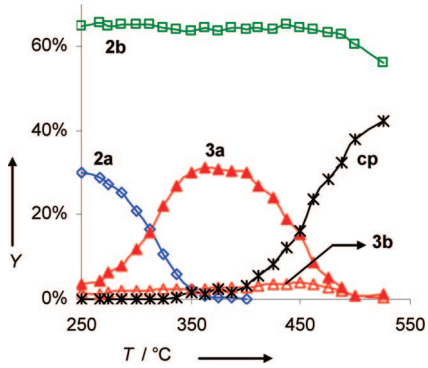

FIGURE 3. Yield of pyrolysis products of ocimene pyrolysis and content of ocimene isomers depending on reaction temperature (*T*). **2a**, 3*Z*-ocimene; **2b**, 3*E*-ocimene; **3a**, 4*E*,6*Z*-alloocimene; **3b**, 4*E*,6*E*-alloocimene; **cp**, consecutive products. 15 μL starting material; carrier gas, N_2; flow rate, 1.0 L min^{-1}; τ, 0.51−0.78 s.

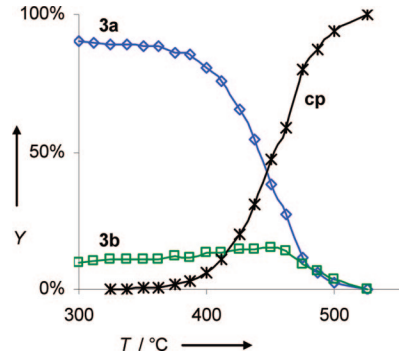

FIGURE 4. Content of alloocimene isomers and yield of its pyrolysis products depending on reaction temperature (*T*). **3a**, 4*E*,6*Z*-alloocimene; **3b**, 4*E*,6*E*-alloocimene; **cp**, consecutive products. 15 μL starting material; carrier gas, N_2; flow rate, 1.0 L min^{-1}; τ, 0.51−0.71 s.

Therefore the low yields reported for **2** (Figure 1) in the case of the pyrolysis of **1** have to be assigned to the formation of **2b**, because at those temperatures the *Z*-isomer is not present any more. Additionally the temperature dependence of the yields of pyrolysis products of **2** are shown, indicating that alloocimene (**3**) is formed in two stereoisomeric forms, 4*E*,6*Z*- (**3a**) and 4*E*,6*E*-alloocimene (**3b**, Chart 1), whereby **3a** is the main product. After passing through a maximum at 375 °C the yield of **3a** decreases in favor of the formation of consecutive products (**cp**), whereas the amount of **3b** formed from **2a** remains constant. Structures of the two alloocimenes were confirmed by comparison of retention times and mass spectra with those of an authentic mixture of **3a** and **3b**. ^{1}H NMR spectra in combination with NOE-experiments with this authentic sample allowed for structural elucidation of the two isomers (cf. Supporting Information).

CHART 1. Structures of 3*Z*-Ocimene (2a), 3*E*-Ocimene (2b), 4*E*,6*Z*-Alloocimene (3a), and 4*E*,6*E*-Alloocimene (3b)

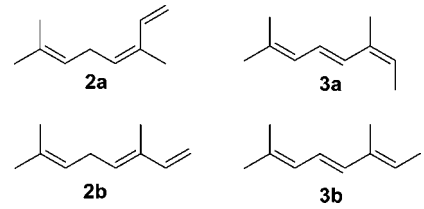

Pyrolysis of Alloocimene. Pyrolysis experiments with a mixture of **3a** and **3b** were conducted in order to investigate the thermal behavior of these two diastereomers (**3a**/**3b**: 9.0). As described, the pyrolysis of **2a** yields those two isomers in favor of **3a**. Figure 4 reports the dependency between reaction temperature and the molar ratio of **3a** and **3b**, revealing that both were converted into other $C_{10}H_{16}$ hydrocarbons (**cp**; e.g., pyronenes).[10] Because of the fact that aromatization and decomposition of those consecutive products occurred at temperatures higher than 525 °C, this region was not investigated in detail.[18] Contrary to **3a**, the content of **3b** seems to increase slightly until 450 °C and after passing through this maximum decreases in the same way as observed for the 4*E*,4*Z*-isomer **3a**, thus indicating that isomerization of **3a** to the other isomer takes place.

Pyrolysis experiments with **1** and its acyclic pyrolysis products **2** and **3** reveal significant differences with respect to the temperature region they are converted. Comparison of these results allows for the conclusion that **2a** is the most reactive isomer and **3** the most thermally stable $C_{10}H_{16}$ hydrocarbon. Results confirm the findings that **2a** is only present in very low concentrations in the mixture of pyrolysis products yielded from thermal isomerization of **1**.[4,5,9,10,19]

Elucidation of Kinetic Steps in the Pyrolysis of α-Pinene. α-Pinene (**1**) as well as its acyclic main isomerization products 3*Z*-ocimene (**2a**), 4*E*,6*Z*-alloocimene (**3a**), and 4*E*,6*E*-alloocimene (**3b**) were subjected to kinetic studies. The simplified reaction scheme used for calculation of the rate constants k_i is depicted in Scheme 2. Explorative pyrolysis studies revealed that **1** primarily isomerizes to give **2a** and **4**, whereby minor amounts of 3*E*-ocimene (**2**: < 2.5%; Figure 1) were neglected

(18) (a) Parker, E. D.; Goldblatt, L. A. *J. Am. Chem. Soc.* **1950**, *72*, 2151–2159. (b) Crowley, K. J.; Traynor, S. G. *Tetrahedron Lett.* **1975**, *16*, 3555–3558. (c) Crowley, K. J.; Traynor, S. G. *Tetrahedron* **1978**, *34*, 2783–2789.

(19) Pascual Teresa, J. de.; Sanchez Bellido, I.; Alberdi Albistegui, M. R.; Feliciano, A. san.; Grande Benito, M. *Anal. Quim.* **1978**, *74*, 301–304; CAN 89:163752.

SCHEME 2. Simplified Reaction Network Used for Calculation of Rate Constants k_{1-7}

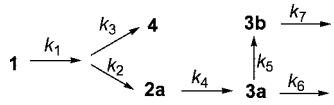

TABLE 1. Kinetic Data[a] for the Gas-Phase Isomerization Reactions of α-Pinene (1; k_{1-3}), 3*Z*-Ocimene (2a; k_4), and Alloocimene (3; k_{5-7}; cf. Scheme 2)

	E_a (kJ mol^{-1})	log A (s^{-1})	$\Delta H^{\ddagger}$ (kJ mol^{-1})	$\Delta S^{\ddagger}$ (J K^{-1} mol^{-1})
k_1	170.0 ± 1.7	13.70 ± 0.14	165.2 ± 1.6	3.0 ± 0.04
k_2	178.5 ± 1.8	14.11 ± 0.15	173.7 ± 1.8	11.0 ± 0.2
k_3	160.8 ± 2.4	12.61 ± 0.19	155.9 ± 2.3	−17.7 ± 0.4
k_4	125.72.1	11.31 ± 0.18	120.8 ± 2.1	−42.4 ± 1.0
k_5[b]	181	12.4	175	−23
k_6	150.9 ± 7.4	11.18 ± 0.54	144.9 ± 7.3	−46.6 ± 3.2
k_7	242.4 ± 7.6	17.49 ± 0.55	236.4 ± 7.6	74.3 ± 2.9

[a] Error limits are 95% certainty limits. [b] Based on experiments at only two different temperatures.

due to its thermal stability within the temperature range investigated (250−525 °C; Figure 3). It has to be pointed out that the network presented in Scheme 2 does not include the reaction(s) leading to racemized **1**. Consideration of the gas-phase racemization of both enantiomers of **1** within the simplified model described in Scheme 2 is difficult from various points of view. As reported in Figure 2, both (−)-**1** and (+)-**1** undergo beside their racemization isomerization reactions leading to **2** and racemic **4** as primary pyrolysis products with selectivities being independent from the enantiomer used. This allows for the conclusion that both molecules take part in the isomerization reaction, and therefore it seems to be impossible to combine the kinetics for rearrangement and racemization. Combination of both processes would lead to rate equations with feedback routes because if molecules of (+)-**1** are formed from the respective (−)-enantiomer those can either undergo isomerization or can be reconverted to give (−)-**1**.

Arrhenius as well as Eyring activation parameters were calculated according to eqs 1 and 2, respectively. Pyrolysis experiments with pure **1** and with mixtures of diastereomeric **2** and **3** were conducted to determine the rate constants k for the disappearance of **1** (k_1), **2a** (k_4), **3a** (k_5, k_6), and **3b** (k_7). On the basis of these data it was possible to calculate the other rate constants using the model of competitive parallel first-order reactions. Activation data are summarized in Table 1. Hence, in the case of calculation of k_5, experiments at only two different temperatures were able to be considered and no error limits are given. Rate constants and Arrhenius plots are given in Supporting Information.

$$k_T = A \cdot e^{-\frac{E_a}{RT}} \quad (1)$$

$$k_T = \frac{k_B T}{h} \cdot e^{-\frac{\Delta H^{\ddagger} - T\Delta S^{\ddagger}}{RT}} \quad (2)$$

Consideration of log A together with $\Delta S^{\ddagger}$ allows for characterization of the transition states the reactions presumably pass through. Typical parameters for "normal" transition states are approximately 13 in log A and activation entropies of around 0 J K^{-1} mol^{-1} as found for k_1 describing the disappearance of **1**. Literature assumes that those transition states have a similar geometry as the ground-state geometry of the starting molecule with minor differences in torsional and rotational degrees of movement.[20] Hence, "normal" transition states are reported to be typical for fragmentations of four-membered rings the results found herein for k_1 are in accordance to those from studies investigating the thermal decomposition of cyclobutane derivatives.[20−23] Similar conclusions can be drawn for the formation of **2a** from **1** (k_2; Table 1), but the positive activation entropy in this case is an indicator for a "loose" transition state being typical for biradical intermediates the reaction passes through. Therefore, it seems to be appropriate assuming that both reactions k_1 and k_2 are reactions involving biradical intermediates. A high Arrhenius factor and an activation entropy of 74 J K^{-1} mol^{-1} were found for the reaction describing the disappearance of **3b** (k_7) being an unequivocal indicator for the fact that this reaction passes through (a) radical reaction intermediate(s). In contrast to **3b** the activation parameters for the disappearance of the 4*E*,6*Z*-isomer of **3a** (k_6; Table 1) are typical for reactions passing through rigid six-membered ring transition states. These are characterized by a lower degree of freedom for torsional and/or rotational movement.[20] Therefore it can be concluded, that beside k_7 the formation of **4** from **1** (k_3), the isomerization of **2a** to **3a** (k_4), and the reaction of **3a** leading to **3b** (k_5) are reactions passing through six-membered ring transitional states (e.g., [1,5]H-shift, ene reaction).

TABLE 2. Rate Constants for the Formation of Ocimene (k_2) at 350 °C Calculated from the Arrhenius Activation Parameters

reaction conditions	E_a (kJ mol^{-1})	log A (s^{-1})	k_2 (s^{-1})	ref
glass ampoules, liquid phase	178.6	15.6	4.261	8a
glass ampoules, liquid phase, N_2	171	13.30	0.093	9
batch reactor, gas phase, vacuum	181.3	14.1	0.080	10
flow-type reactor, supercritical ethanol[a]	136.6			14, 24
flow-type reactor, N_2	178.5	14.11	0.137	this work

[a] Activation energies calculated on the basis of a model of the reactor used for the experiments.

The thermal isomerization reaction of **1** was subject of various kinetic pyrolysis studies performed in gaseous, condensed, or supercritical phase.[5,8a,9,10,14,24] Comparison of the kinetic data presented in Table 1 with those reported in the literature reveals a high accordance. Although the network of reactions based on pyrolysis of **1** has been subjected to kinetic studies since the 1950s, there is only one study investigating the isomerization of **1** in the gas phase using a flow-type reactor.[5] Unfortunately, this study reported data for the isomerization of **2a** leading to **3** (k_4) only. Nevertheless, these results are in agreement with those reported herein and found for pyrolysis experiments in the liquid phase.[9,11] Respective rate constants for the formation of **2a** from **1** (k_2) on the basis of the reported Arrhenius parameters for 350 °C are listed in Table 2. Only the studies of Fugitt and Hawkins performed in glass ampoules under noninert conditions led to a higher rate constant, which might indicate that the reaction is not independent from pressure under those conditions applied. This fact seemed to be proveed with respect to the studies of Anikeev and co-workers using supercritical ethanol in a flow system as fluid.[14,24] Activation energies, E_a,

(20) (a) Gowenlock, B. G. *Quart. Rev.* **1960**, *14*, 133–145. (b) Walsh, R. *Chem. Soc. Rev.* **2008**, *37*, 686–698.
(21) Wellman, R. E.; Walters, W. D. *J. Am. Chem. Soc.* **1957**, *79*, 1542–1546.
(22) Frey, H. M.; Walsh, R. *Chem. Rev.* **1969**, *69*, 103–124.
(23) Chickos, J. S.; Frey, H. M. *J. Chem. Soc., Perkin Trans. 2* **1987**, 365–370.
(24) Yermakova, A.; Chibiryaev, A. M.; Kozhevnikov, I. V.; Anikeev, V. I. *J. Supercrit. Fluids* **2008**, *45*, 74–79.

calculated on this basis showed significant differences from all other values reported in Table 2. Obviously, other reaction mechanisms are present when the reaction is carried out in a high-pressure regime. Differences of the rate constant calculated on the basis of the vacuum pyrolysis studies by Gajewski and co-workers (0.0013 mbar, static system) may be due to the fact that k are not pressure-independent anymore.[10] In general rate constants were observed to be generally independent from total pressure at pressure greater than 1 atm, whereas at lower pressures the rate constants "fall off" and the activation mechanism is changed. Reactions performed under (V)LPP-conditions without an additional fluent have a different activation procedure, because the collisions between reactant molecules can not be ignored. Therefore, often the rate constant of the rate-determining step is of second-order for the falloff region rather than (pseudo)-first-order.[25] Activation parameters available from literature for the disappearance of **3**[9,10] indicate that mostly **3a** is formed from **2a**, thus being in agreement with the pyrolysis studies on **2** and **3** presented in Figures 3 and 4.

Pyrolysis Mechanisms of α-Pinene, Ocimene, and Alloocimene. Pyrolysis experiments as well as kinetic analysis of the most important reactions in the thermal reaction network based on **1** allow for mechanistic evaluation of the initial reaction steps. Pyrolyses with **1** (Figure 1) reveal that the ratio of primary formed pyrolysis products **2** and **4** remains constant while increasing temperature and conversion of **1** from 300 to 500 °C or 0 to 100%, respectively. This behavior is reported to be not atypical for reactions passing through the same intermediate or transition state.[15] Additionally, enantiomerically pure (−)-**1** as well as (+)-**1** were subjected to pyrolysis studies in order to investigate the temperature dependency of the enantiomeric excess (Figure 2), revealing that racemization occurred independently from the enantiomer used as starting material. This allows for the conclusion that three major reactions contribute to the disappearance of **1** during its thermally induced rearrangement: racemization of **1**, fragmentation of the cyclobutane ring (**2**, **3**, **cp**), and the formation of dipentene (**4**).[10] Those set of reactions are reported to be typical for isomerization of vinylcylobutanes.[23,26] According to the theoretical study of Northrop and Houk on vinylcyclobutane rearrangement, only the *syn*-conformer has the ability to undergo [1,3] carbon shift to cyclohexene and fragmentation to *cisoid*-butadiene and ethylene, whereas the *anti*-isomer formed *transoid*-butadiene and ethylene only. Additionally cyclohexene is able to form butadiene and ethylene via retro-Diels−Alder reaction.[26g] Hence, **1** is a bridged bicyclic vinylcyclobutadiene with *cis*-orientation both reaction pathways are virtually possible. Kinetic analysis of the reactions responsible for disappearance of **1** (k_1) and the formation of **2a** (k_2) and **4** (k_3; cf. Scheme 2 and Table 1) allows for the conclusions that k_1 and k_2 pass through "loose" transition states, whereas the reaction leading to product **4** runs through a six-membered ring transition state. Since [2 + 2]-cycloadditions as well as [2 + 2]-cycloreversions are thermally forbidden reactions with respect to the Woodward−Hoffmann rules,[27]

SCHEME 3. Reaction Network of α-Pinene Thermal Isomerization

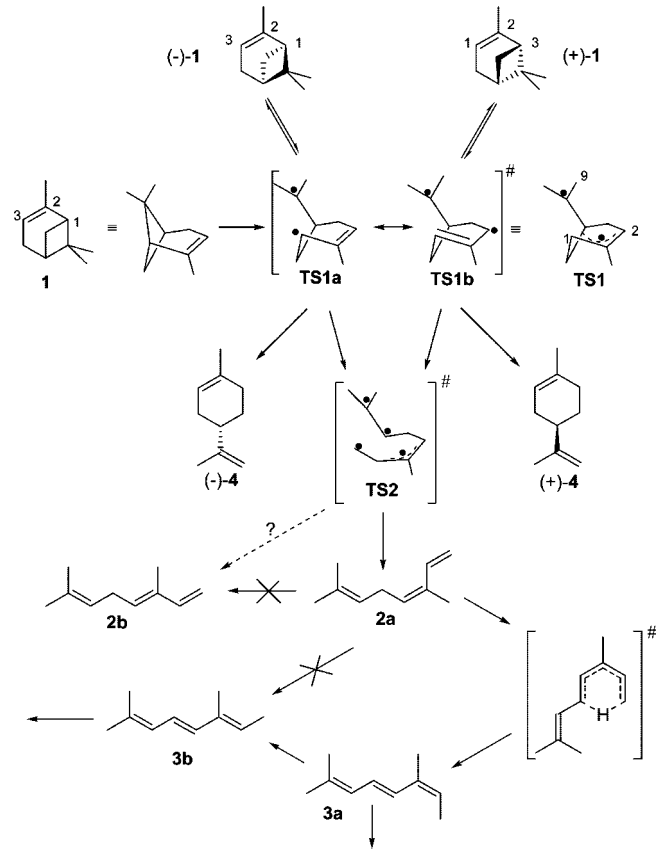

formation of **2a** has to proceed stepwise including a biradical intermediate depicted in Scheme 3.[6,10,28]

On the basis of the initially formed biradicals, three possible reaction pathways exist leading to the formation of products **2a**, **4**, and to racemized **1**. Reconnection of the bond initially been broken in the case of **TS1a** leads to **1** with the initial configuration, whereas bond reformation in **TS1b** yields the opposite enantiomer. This racemization reaction can be classified as 1,3-sigmatropic rearrangement reaction. Literature reports many examples for similar thermally as well as photochemically induced isomerizations.[26d,e,29]

Analysis of the resulted pyrolysis products from thermal isomerization experiments of both enantiomers of **1** reveals that racemic **4** (dipentene) is formed independently from temperature, conversion of **1**, and from the initial enantiomeric excess (Figure 2). Obviously the mesomeric delocalization of the initially formed biradical is fast compared to its consecutive reactions, implying that the change of hybridization of C(1) is not rate-

(25) Gajewski, J. J. *Hydrocarbon Thermal Isomerization*, 2nd ed.; Elsevier Academic Press: London, 2004; pp 1−3.

(26) (a) Frey, H. M.; Walsh, R. *Chem. Rev.* **1969**, *69*, 103–124. (b) Gajewski, J. J.; Paul, G. C. *J. Am. Chem. Soc.* **1991**, *56*, 1986–1989. (c) Lewis, D. K.; Charney, D. J.; Kalra, B. L.; Plate, A.-M.; Woodard, M. H.; Cianciosi, S. J.; Baldwin, J. E. *J. Phys. Chem. A* **1997**, *101*, 4097–4102. (d) Leber, P. A.; Baldwin, J. E. *Acc. Chem. Res.* **2002**, *35*, 279–287. (e) Baldwin, J. E. *Chem. Rev.* **2003**, *103*, 1197–1212. (f) Baldwin, J. E.; Leber, P. A. *Org. Biomol. Chem.* **2008**, *6*, 36–47. (g) Northrop, B. H.; Houk, K. N. *J. Org. Chem.* **2006**, *71*, 3–13.

(27) (a) Woodward, R. B.; Hoffmann, R. *Angew. Chem., Int. Ed.* **1969**, *8*, 781–853. (b) Hoffmann, R.; Woodward, R. B. *Science* **1970**, *167*, 825–831. (c) Ponec, R. *Top. Curr. Chem.* **1995**, *174*, 1–26.

(28) (a) Stolle, A.; Ondruschka, B.; Bonrath, W. *Eur. J. Org. Chem.* **2007**, 2310–2317. (b) Stolle, A.; Ondruschka, B.; Findeisen, M. *Proceedings of the 3rd International Conference on Environmental Science and Technology, Houston, TX, August 5−9, 2007*; Starrett, S. K.; Hong, J.; Wilcock, R. J.; Li, Q.; Carson, J. H.; Arnold, S., Eds.; American Science Press: Houston, 2007; pp 325−329.

(29) (a) Frey, H. M.; Hopkins, R. G.; O'Neal, H. E. *J. Chem. Soc., D* **1969**, 1069. (b) Roth, W. R.; Friedrich, A. *Tetrahedron Lett.* **1969**, *10*, 2607–2610. (c) Roth, W. R.; König, J.; Stein, K. *Chem. Ber.* **1970**, *103*, 426–439. (d) Schuster, D. I.; Widman, D. *Tetrahedron Lett.* **1971**, *12*, 3571–3574. (e) Dietrich, K.; Musso, H. *Chem. Ber.* **1974**, *107*, 731–734. (f) Gajewski, J. J. *Hydrocarbon Thermal Isomerization*, 2nd ed.; Elsevier Academic Press: London, 2004; pp 46−50.

SCHEME 4. Thermal Network of Pyrolysis Products from Thermolysis of 2,2-Dimethyl-1-vinylcyclobutane (5) and Its Relationship to α-Pinene (1)[a]

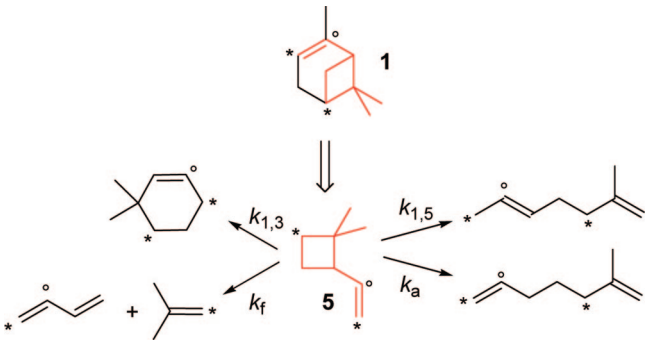

[a] Asterisks attached to **5** and its pyrolysis products assign connection points for the cyclohexane ring in **1**, whereas the circle assigns the missing methyl group.[23]

determining; otherwise optically active **4** has to be formed. Additionally the *syn*-configuration of the vinylic system remained unchanged since the change of configuration to *anti* in the cyclic system would lead to an intermediate with *trans*-cyclohexene structure, which is energetically disfavored.[26g]

Activation parameters for the formation of dipentene from **1** indicate a "tight" transition states thus implying a [1,5]H-shift reaction as most plausible reaction (Scheme 3).[10] Because racemic **4** is formed, the retro-ene reaction has to proceed after the formation of the biradical rather than before. Retro-ene reaction of the starting material would yield optically active **4**. Since in the biradical intermediates **TS1a** and **TS1b** the one radical is delocalized as allyl-type radical, **TS1** loses completely its configurational integrity as a result of the existence of a mirror plane (point symmetry group: C_S). Due to the findings presented in Figure 2 it is obvious that the formation of **4** is faster than racemization of **1**. This leads to the conclusion that the reconnection of the carbon bond is unfavorable comparing to the hydrogen shift, thus indicating that the isopropyl group changes its confirmation during the formation of the radical intermediates.

The formation of **2a** from **1** by thermally induced rearrangement follows the known mechanisms for ring opening of cyclobutanes.[21−23,29f,30] Rupture of the second carbon−carbon bond in intermediate **TS1** and subsequent radical recombination yielded 3*Z*-ocimene (**2a**) exclusively. The formation of **2b** is suppressed because of the rigid cyclic structure in the case of **TS1**. The small amounts of the *E*-isomer (**2b**) probably result from transition state **TS2**, whereby rotation around the C(2)−C(3) single bond seems to be the most plausible explanation, which indicated that the mesomeric delocalization is not complete, since a rotation around a C−C-bond with sp^2-hybridized atoms is impossible. However, a photochemical rearrangement of **2a** to **2b**[31] can be ruled out due to the absence of any quenchers and the stability of a mixture of both diastereomers.

Results reported herein on the pyrolysis of **1** are in good agreement with thermolysis studies on 2,2-dimethyl-1-vinylcyclopropane (**5**) as nonbridged cyclobutane model for **1**.[23] The relationship between **1** and **5** is described in Scheme 4. Asterisks attached to **10** and its pyrolysis products assign connection points for the cyclohexane ring in **1**, whereas the circle assigns the

CHART 2. Possible Transition States (TS3a and TS3b) for the Formation of 4*E*,6*Z*-Alloocimene (3a) from 3*Z*-Ocimene (2a)[11]

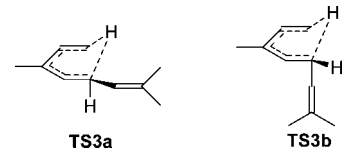

missing methyl group. Four major reaction pathways were found by Chickos and Frey indicated by the respective rate constants in Scheme 4. Fragmentation of **5** (k_f) yields isobutene and 1,3-butadiene exclusively, whereby the addition of the missing methylene bridge and methyl group leads to **2a**. 4,4-Dimethylcyclohexene is the 1,3-sigmatropic shift reaction product ($k_{1,3}$) from **5** being equal to the racemized form of **1** after pyrolysis. Both reaction pathways leading to acyclic products for the pyrolysis of **5** differ in position of one of the two carbon−carbon double bonds, thus expressing the two different enantiomers of **4** resulting from pyrolysis of **1**. Comparison of experimental results presented herein and those found for thermolysis of **5**[23] showed a good agreement concerning the products formed and therefore the comparability of the two compounds.

Results of pyrolysis experiments with a mixture of 3*Z*- (**2a**) and 3*E*-ocimene (**2b**) depicted in Figure 3 revealed that predominately the *Z*-isomer was isomerized, whereas the concentration of **2b** remains constant within the temperature range investigated. Analysis of the pyrolysis products revealed that the formation of 4*E*,6*Z*-alloocimene (**3a**) is favored, whereby thermolysis experiments with a mixture of **3a** and **3b** allows for the conclusion that the 4*E*,6*E*-isomer (**3b**) results from reconfiguration of the 6*Z*-double bond in **3a**. Therefore, the conclusion can be drawn that both the formation of **2a** and its disappearance are highly diastereospecific reactions. Liquid-phase pyrolysis studies with **2a** reported similar activation parameters found for the gas-phase isomerization presented in Table 1 (k_4).[11] Activation entropy $\Delta S^{\ddagger}$ and frequency factor log *A* indicate a "tight" transition state as reaction intermediate, being typical for reactions passing through a six-membered ring transition state.[20] Probably, the rearrangement of **2a** to **3a** proceeds as [1,5]H-shift reaction pictured in Scheme 3. According to the Woodward−Hoffmann rules, this reaction is thermally allowed if it proceeds in the suprafacial version.[11,22,27,32] Whereas the stereospecific formation of the 6*Z*-double bond in **3a** is due to the rigid cyclic transition state, the stereochemistry of the double bond at C(4)−C(5) is controlled by the nature of the reaction intermediate. Chart 2 pictures two possible intermediates (**TS3a** and **TS3b**) for the suprafacial [1,5]H-migration leading to either **3a** or to 4*Z*,6*Z*-alloocimene, respectively. It is evident that the thermal isomerization of **2a** exclusively yields **3a** and the reaction has to pass through intermediate **TS3a** (Chart 2). The preference of **TS3a** to **TS3b** could be explained by less steric repulsion of the large isobutenyl substituents in the less crowded equatorial position than in the more crowded axial.[11]

The formation of **3b** from **3a** can be explained by acid- or base-catalyzed rearrangement of the respective double bond affected by interactions with the reactor walls. This is evident with respect to the kinetic analysis of the temperature-dependent yields of both stereoisomers of **3** reported in Figure 4. On the basis of the activation parameters listed in Table 1 for the rate

(30) Srinivasan, R.; Kellner, S. M. E. *J. Am. Chem. Soc.* **1959**, *81*, 5891–5893.
(31) Frank, G. *J. Chem. Soc., B* **1968**, 130–132.
(32) Mironov, V. A.; Fedorovich, A. D.; Akhrem, A. A. *Russ. Chem. Rev.* **1981**, *50*, 666–681.

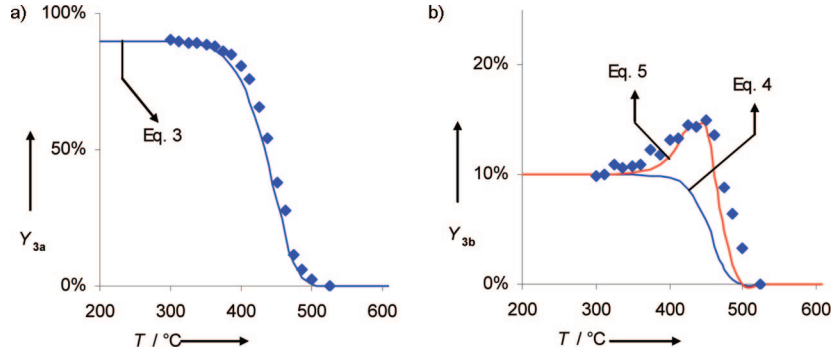

FIGURE 5. Comparison of data for the temperature-dependent contents of 4*E*,6*Z*-alloocimene (Y_{3a}; Figure 5a) and of 4*E*,6*E*-alloocimene (Y_{3b}; Figure 5b) from experiment (◆; cf. Figure 4a) and for data based on kinetic parameters listed in Table 1.

constants k_5, k_6, and k_7 (Scheme 2) and with respect to eq 1 it is possible to calculate the mole fractions of **3a** and **3b**. Assuming that a mixture of both isomers is used (**3a**/**3b** = 9.0), eqs 3 and 4 allow for the calculation of their concentrations at a desired temperature and residence time, respectively. The additional formation of **3b** from **3a** is neglected in this first step of approximation.

$$[\mathbf{3a}]_T = [\mathbf{3a}]_0 \cdot e^{-k_{6;T}\tau} = 0.9 \cdot e^{-k_{6;T}\tau} \quad (3)$$

$$[\mathbf{3b}]_T = [\mathbf{3b}]_0 \cdot e^{-k_{7;T}\tau} = 0.1 \cdot e^{-k_{7;T}\tau} \quad (4)$$

Figure 5a reveals that this simple kinetic is able to describe well the disappearance of the 4*E*,6*Z*-isomer, whereas it is not suitable for the modeling in the case of **3b** (Figure 5b). It is evident that consideration of the side reaction describing the isomerization of **3a** to **3b** (eq 5) allows for an excellent modeling of the temperature-dependent content of **3b** (Y_{3b}; cf. red line in Figure 5b). Therefore, this *Z*/*E*-isomerization of the two isomers of alloocimene is approved to proceed as a one-directional reaction. Other isomers of **3** with a *Z*-configuration of the carbon−carbon double bond at C(4)−C(5) were not able to be identified in the reaction mixture, thus being in accordance with the proposed mechanism pictured in Scheme 3. Consecutive reactions of both isomers of **3** yield various monocyclic products that mainly result from cyclization reactions leading to substituted cyclohexadienes, thus being in agreement with the reported activation data listed in Table 1 for the disappearance of **3** (k_6, k_7).[18]

$$[\mathbf{3b}]_T = \left[[\mathbf{3b}]_0 + \frac{[\mathbf{3a}]_0 \cdot k_{5;T}}{k_{6;T}}(1 - e^{-k_{6;T}\tau})\right] \cdot e^{-k_{7;T}\tau}$$
$$= \left[0.1 + \frac{0.9 \cdot k_{5;T}}{k_{6;T}}(1 - e^{-k_{6;T}\tau})\right] \cdot e^{-k_{7;T}\tau} \quad (5)$$

Conclusion

The bicyclic monoterpene α-pinene (**1**) was subjected to gas-phase pyrolysis studies. Carrier gas pyrolysis of **1** reveals that in addition to racemization of the starting material the formation of alloocimene (**3**) and racemic limonene (**4**) was observed. The expected product from ring opening of the cyclobutane ring in **1**, ocimene (**2**) was not present in the product mixtures, thus indicating that it is a highly reactive compound. In order to unravel primary from secondary pyrolysis products, thermal isomerization experiments with **2** and **3** were conducted. Obviously the isomerization of 3*Z*-ocimene (**2a**) yields 4*E*,6*Z*-alloocimene (**3a**) exclusively. The 3*E*-isomer (**2b**) is thermally stable, and only minor amounts found in the pyrolysis product of **1** seem to result from undesirable side reactions. Reactions of **2a** directly leading to **2b** or 4*E*,6*E*-alloocimene (**3b**) were not found. Results are summarized in the thermal reaction network presented in Scheme 3. Products primarily formed from **1** are in agreement with those resulting from pyrolysis of 2,2-dimethyl-vinylcyclobutane.

Kinetic analysis of the reactions allowed for determination of Arrhenius as well as Eyring activation parameters for the initial reaction steps. The use of nitrogen as carrier gas allows for performing the reaction apart from the falloff region. Because of the high extent of this diluting agent, its concentration relative to substrate molecules is constant, allowing for the assumption that the rate-determining reaction steps are unimolecular. The model of competitive first-order parallel and consecutive reactions was used to describe the reaction network. Activation entropies and frequency factors for the formation of **2a** and the racemization of **1** clearly indicate a biradical as transition state. This is in accordance with the rules of Woodward and Hoffmann, because [2 + 2]-cycloreversions are thermally forbidden reactions. Therefore, the fragmentation of the cyclobutane ring has to proceed stepwise. The formation of racemic **4** and the fast isomerization of **2a** to **3a** seem to proceed as [1,5]H shift reactions. Activation energy for the disappearance of **2a** supports the hypothesis that this is a very reactive molecule. Pyrolysis of a mixture of **3a** and **3b** indicate an isomerization leading from **3a** to **3b** but not the other way.

Experimental Section

Pyrolysis Experiments. Dilution gas pyrolyses were carried out in an electrically heated quartz tube 500 mm in length and with a pyrolysis zone approximately 200 mm in length, using the apparatus reported previously.[16] Temperatures (T) were regulated with thermocouples, and in addition the actual T was measured inside the reactor. In all experiments, oxygen-free nitrogen with a purity of >99.999% was used as the carrier gas. The substrates (15 μL) were introduced onto a quartz ladle at the top part of the pyrolysis apparatus using a glass syringe (50 μL) and carried along with the nitrogen stream into the reactor. Vaporization of the starting material was supported by heating the ladle to 200 °C with a hot blast. Pyrolysis products were collected in a cold trap (liquid nitrogen) and were dissolved in 1.5 mL of ethyl acetate.

The liquid products obtained were analyzed by GC-FID and GC-MS, with 5 μL of hexadecane added as internal standard. Comparison of both residence times and mass spectra with those of reference compounds allowed for identification of the main

products. Yields and conversions have been calculated on the basis of the corrected and normalized peak areas from the GC analyses.

Kinetic Experiments. The kinetic experiments were carried out in different temperature ranges depending on the starting materials used for the experiments. Lower and upper boundaries for the experiments were chosen with respect to those regions in the respective temperature−conversion plots where the slope of the curve is linear. Variation of the carrier gas velocity in a range from 0.4 to 1.2 L min^{-1} N_2 allowed for the modulation of the average residence time (τ). Pyrolysis experiments used for calculation of rate constants were individually carried out three times. For calculation of the parameters, all experimental results were considered. If outliers were present within a data set the corresponding experiments were redone individually four times and the data were recalculated considering the additional experiments. Determination of various rate constants by performing kinetic pyrolysis experiments at various temperatures allows for the calculation of both Arrhenius (E_a, log A) as well as Eyring activation parameters ($\Delta H^{\ddagger}$, $\Delta S^{\ddagger}$; eqs 1 and 2).

Supporting Information Available: Analytical details, calculation procedure for residence time, pyrograms of the three substrates (**1**, **2**, **3**), 1D-NOESY data for structural elucidation of isomeric ocimenes and alloocimenes, rate constants for all reactions shown in Scheme 2, and Arrhenius plots for the calculation of the activation parameters. This material is available free of charge via the Internet at http://pubs.acs.org.

JO8012995